Vibration modeling of magnetic tape with vibro-impact of tape–guide contact

John M. Boyle Jr, Bharat Bhushan*

Nanotribology Laboratory for Information Storage and MEMS/NEMS, Department of Mechanical Engineering, The Ohio State University, Columbus OH 43202, USA

Abstract

Next-generation, high track-density linear tape drives will require improved tape guiding and dimensional stability in order to achieve better performance and higher storage capacities. Drive vibrations, tape degradation, debris formation, and tape guiding all contribute to unwanted lateral tape motion (LTM), which can lead to track-misregistration errors during reading of the tape. Understanding the nature of LTM is of prime interest. A nonlinear vibration model of a tape–guide system with vibro-impact is presented in this study. The guides are modeled as rigid constraints, while the reels are modeled as clamped ends. Free vibration (due to initial velocity) and forced vibration (due to moving boundaries) were performed for various test cases to determine the effect of tape tension and thickness, tape–guide separation distance, reel tilt amplitude, and tape speed. The model results are compared to actual experimental LTM data, though with the absence of tape damping and tape–guide frictional forces in the model, only limited comparisons may be made.
© 2005 Elsevier Ltd. All rights reserved.

1. Introduction

Linear tape drives operate by routing magnetic media through a system of reels and guides past a recording head in a serpentine fashion. This multi-billion dollar industry is poised to undergo radical changes in drive operation and storage capacity that will require a new understanding of

*Corresponding author. Tel.: +1 614 292 0651; fax: +1 614 292 0325.
E-mail address: bhushan.2@osu.edu (B. Bhushan).

performance issues such as tape speed, tension, and thickness. Next-generation high track-density linear tape drives will require a more stable tape path due to these technological advances. Increasing demands for higher storage capacity is forcing the use of thinner tapes, lower track width, and higher tape speeds for future high-performance linear tape systems [1,2].

As more tracks are added to the tape, the need for better guiding systems and tape dimensional stability arises. Without better guiding and dimensional stability, unwanted lateral (transverse) tape motion (LTM) can occur, causing a track-misregistration (TMR) error. TMR occurs when lateral motion causes the data tracks on the tape to incorrectly align with read–write elements on the head. To prevent improper data recording, the head ceases writing and a TMR error is signaled [3,4]. Modern tape drives utilize magnetic head servoactuators to counter long-wavelength LTM. However, these head tracking servos have limited bandwidth. High-frequency LTM above 1 kHz is outside of the servo bandwidth and cannot be adequately compensated at this time due to inertia of the head [5].

The origin of LTM can be attributed to several sources. Due to factory slitting, the magnetic tape edge is not smooth (uniform) [6–10]. The edges are rough and comprised of many asperities that can impact the guide flanges of the tape drive, forcing the tape into transverse motion. The mechanical vibrations of the drive itself, due mainly to reel rotation, is yet another source of unwanted transverse motion. Staggered wraps in the tape pack can also be a source of LTM as the tape unwinds. Finally, debris formation at the guides or head can become lodged between the tape and the drive interfaces, possibly forcing the tape into transverse motion due to the impact.

In reality, LTM is not the only source of unwanted movement during tape drive operation. In addition to lateral motion, the tape could vibrate axially or twist about its centerline in a cupping motion. LTM was chosen as the primary focus of study due to its high relevance as a major contributor to TMR errors and its relative ease of measurement compared to other tape motions [9–11]. LTM has been measured extensively in the past, but there are relatively few published theoretical models to predict transverse motion.

During unwinding, any reel imbalance may impart an edge force onto the tape during operation, causing the tape to experience a jump in LTM. Reel tilt amplitude due to reel axial runout (imperfections in reel construction) or improper reel alignment can serve as a harmonic force input for vibrations. Staggered winds in the tape pack can also cause edge forces to influence tape motion [2,9–11]. If the lateral vibration amplitude of the resulting tape motion is greater than the distance between the tape edge and guide flanges, tape–guide impacts will occur.

In a recent study [12], LTM and corresponding frequency components were experimentally measured under varying conditions including tape speed, tension, thickness, and number of operating cycles. In addition, the effect of an impulse force applied to the tape edge was investigated. The motivation behind impulse loading is that tape–guide contact can force the tape into excitation and impacting the tape edge can simulate these phenomena. In addition to experimental analysis, a theoretical approach to tape–guide contact and LTM is desired. The objective of the present study is to develop a mathematical model to predict the vibration of magnetic tape subject to several parameters, including tape tension, speed, and thickness, tape–guide clearance, and reel effects. Using Bernoulli–Euler beam theory, the LTM vibration can be modeled. The tape–guide impacts can be investigated by using vibro-impact methods to model the nonlinear vibration of the tape. In reality, buckling of the tape would become an important

issue to examine, but this is not taken into account in this study. The theoretical results are compared to sample experimental LTM data.

2. Theoretical background

2.1. Sources of LTM

The sources of LTM in magnetic tape can be different, however the reels and guides contribute the majority of unwanted vibrations. As tape unwinds from the reels, any slight disturbance could cause LTM to occur. A reel could be tilted on its axis, the reel hub could be imperfect, or reel runout may occur. Any of these sources will cause the tape to experience a periodic side force imparted on it, which would result in errant tape motion. Fig. 1(a) shows the simple case of reel tilt amplitude and its effect on tape guiding. For each revolution the reel will cause displacement of the tape at the reel rotational frequency with magnitude related to the amount of reel tilt and other imperfections of the reel.

Staggered wraps can also cause unwanted tape vibration. During winding, the tape layers may not align properly. Air can become trapped between the tape layers, causing the tape to slide vertically in the tape pack. This will result in some tape layers being shifted relative to the adjacent
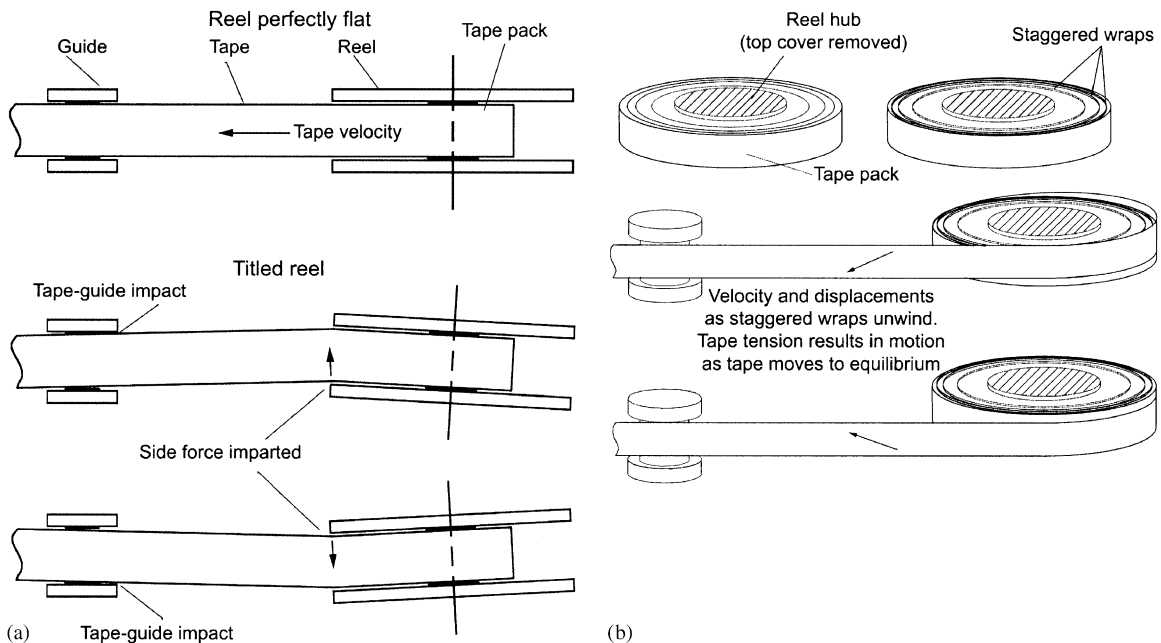

Fig. 1. Schematics to illustrate common sources of LTM. (a) Effect of reel tilt amplitude on tape guiding. Reel and guide misalignment can cause harmonic excitation of the tape and apply side forces to the tape edge, resulting in further unwanted LTM. (b) Effect of staggered wraps on tape guiding. Staggered wraps, formed through improper winding of the tape, can cause very high LTM as the wrap unwinds during operation.

layers in the pack on the reel. Fig. 1(b) shows an illustration of what a staggered wrap looks like in the tape pack. As the wrap unwinds, the tape experiences a very high (magnitude) change in lateral position as the wrap moves toward the equilibrium position of the tape. The larger the staggered wrap, the more severe the resulting transverse velocity and displacement of the tape will be as it unwinds. Damping of the tape will cause the effect of staggered wraps to dissipate, but the initial induced high-LTM will propagate through the tape path causing unwanted motion.

In this study, only the effect of reel tilt amplitude on LTM is studied. Staggered wrap magnitude and frequency are interesting topics to investigate, however the mechanisms behind such motions are not trivial and thus fall beyond the scope of this study.

2.2. Superpositioning of velocity and displacement sources

The effects of tape speed, reel imperfections, and staggered wraps will all contribute to the velocity, V, and displacement, Y, of the tape. Fig. 2 illustrates this point and deconvolves the tape velocity and displacement components into separate sources (Fig. 2(a)). In reality, tape motion is very complicated, but this figure helps illustrate that the end result is a superpositioning of several sources. Each velocity and displacement component can be further deconvolved in order to obtain even more accurate expressions for tape motion (Figs. 2(b) and (c)). In the model, the initial displacement and velocity of the tape would be related to the values of V and Y. In this study, only the effect of an initial transverse velocity at the guide was considered for the free vibration case. For the forced vibration case, no initial conditions were used because beam excitation was in the form of moving boundaries.
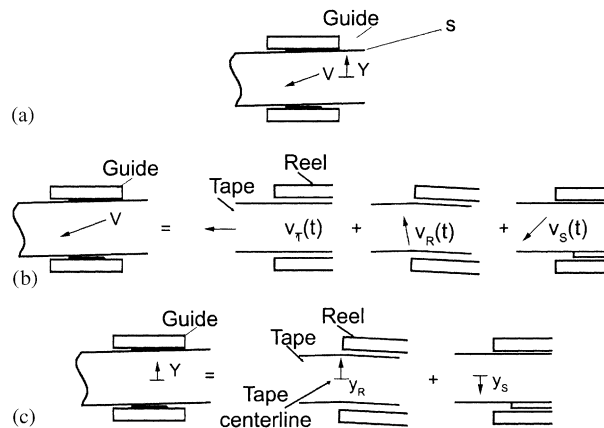

Fig. 2. Superpositioning of velocity and displacement sources. (a) Resultant velocity, V, and displacement, Y, with tape–guide separation distance, s. If Y is greater than s, a tape–guide impact will occur. The magnitude and direction of V, along with the amount of displacement, Y, will determine the nature of the tape–guide impact force. These can be deconvolved into separate components relating to the tape speed, reel effects, and staggered wraps. (b) Velocity components: resultant velocity of the tape due to external sources, $V(t) = v_T(t) + v_R(t) + v_S(t)$, where $v_T(t) =$ linear tape velocity, $v_R(t) =$ velocity due to side force imparted by tilted reel, and $v_S(t) =$ velocity due to equalizing staggered wraps. (c) Displacement components: resultant lateral motion of the tape due to external sources, $Y = y_R + y_S$, where $y_R =$ lateral motion due to side force imparted by tilted reel and $y_S =$ lateral motion due to equalizing staggered wraps.

3. Modeling of LTM

3.1. Modal analysis of clamped–clamped beam

Fig. 3 shows schematics of the tape drive and the reduction to a simple beam model. Fig. 3(a) shows a typical experimental tape drive transport. The tape can be assumed to vibrate as a beam with the nodes at each reel. To show this, Fig. 3(b) depicts the tape transport "unwrapped". If the reels are assumed to be clamped ends and the guides are assumed to be rigid constraints, then the tape can be modeled as a simple beam with the tape–guide clearance of s, the distance between the top of the tape edge and the guide flange (Fig. 3(c)). The zoomed image in Fig. 3(c) shows a close-up of the beam model. Initial conditions based on V and Y of the tape can be applied to the beam
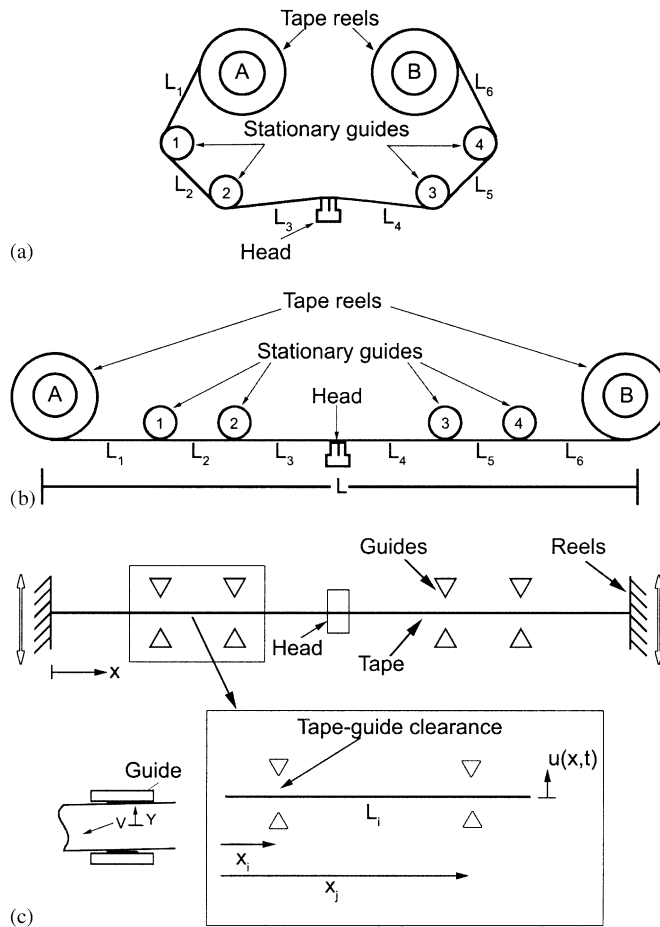
Fig. 3. Reduction of an actual tape drive to a simple beam model. (a) Schematic of actual tape drive. (b) The tape is assumed to behave as a thin beam of length, L. (c) The guides are modeled as rigid constraints with a clearance between the tape and guide. Tape vibration is modeled according to simple Bernoulli–Euler theory. Reels are modeled as clamped ends, but are permitted to move in the lateral direction to simulate uneven winding. $u(x,t) =$ lateral tape motion where the initial conditions are based on V and Y, x_i, $x_j =$ locations of constraints.

and the resulting vibration, $u(x, t)$, can be calculated using a vibration model based on the nonlinear vibro-impacts between the tape and guide if the tape vibration at the guides exceeds the tape–guide clearance [13].

Using separation of variables,

$$u(x, t) = q_i(t)\phi_i(x). \tag{1}$$

The equation for a beam with uniform tension can be written as

$$\phi''''(x) + \alpha\phi''(x) - \beta^4\phi(x) = 0, \tag{2}$$

where $\alpha = -T/(EI)$, $\beta^4 = \omega^2 m/(EI)$, and ω is the natural frequency. The solution to Eq. (2) is found to be

$$\phi(x) = A\,\sin(ax) + B\,\cos(ax) + C\,\sinh(bx)D\,\cosh(bx), \tag{3}$$

where

$$a = \sqrt{\frac{\alpha}{2} + \sqrt{\frac{\alpha}{4} + \beta^4}} \quad \text{and} \quad b = \sqrt{-\frac{\alpha}{2} + \sqrt{\frac{\alpha}{4} + \beta^4}}.$$

Employing the boundary conditions for clamped–clamped ends, $\phi(x)|_{x=0,L} = 0$ and $\frac{d\phi(x)}{dx}|_{x=0,L} = 0$, the characteristic equation is

$$\cos(aL)\cosh(bL) + \frac{a^2 - b^2}{2ab}\,\sin(aL)\sinh(bL) - 1 = 0. \tag{4}$$

The mode shape is

$$\phi(x) = \sin(ax) - \frac{a}{b}\sinh(bx) + a\left(\frac{\cos(aL) - \cosh(bL)}{a\,\sin(aL) + b\,\sinh(bL)}\right)(\cos(ax) - \cosh(bx)). \tag{5}$$

Eq. (4) must be solved for each tape tension and thickness combination to find the appropriate values of β [14].

3.2. Vibration analysis

Fig. 4 shows the location of the constraint along with the location of the head where data was taken. These positions correspond to locations in an actual experimental tape drive system. During tape drive operation, the only LTM that is important to examine is that at the head. Throughout this study, while some results will show LTM at the guide to illustrate the model capabilities, LTM at the head is always presented. Fig. 4(a) shows the beam model with stationary boundary conditions. To study free vibration of the system, an initial transverse velocity of 4 m/s was applied at the guide location. The value of 4 m/s was empirically determined so that the resulting vibration would be of high enough magnitude to cause tape–guide impacts at the constraint. Fig. 4(b) shows beam model with moving boundary conditions due to reel tilt amplitude. $u_g(x, t)$ and $u_h(x, t)$ are the displacements of the beam due to the moving boundaries, represented by

$$u_g(x, t) = \frac{x}{L}\,g(t) = \frac{x}{L}\,a_g\,\sin(\Omega_g t), \tag{6}$$

$$u_h(x, t) = \left(1 - \frac{x}{L}\right)h(t) = \left(1 - \frac{x}{L}\right)a_h\,\sin(\Omega_h t), \tag{7}$$
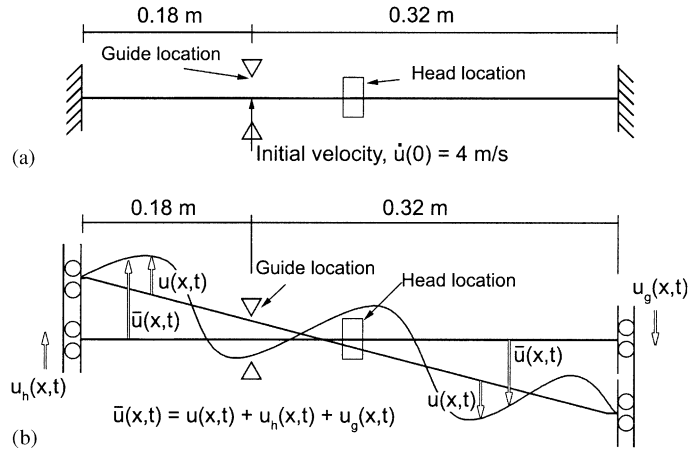
Fig. 4. (a) Model for stationary boundary (free vibration case). Only one guide is modeled and data is simulated at both the guide and head positions. Tape is excited by a 4 m/s initial velocity at the guide. (b) Model for moving boundaries (forced vibration case). One guide is modeled, but instead of an initial velocity, the boundaries move to simulate reel tilt or staggered winds.

where $\Omega_{g,h}$ is the reel rotational frequency, $a_{g,h}$ is the reel tilt amplitude, L is the beam length, and x is the longitudinal beam position. The resulting overall displacement of the tape can be represented by

$$\bar{u}(x, t) = u(x, t) + u_g(x, t) + u_h(x, t). \tag{8}$$

The governing differential equation of motion can then be written as

$$m \frac{\partial^2 \bar{u}(x, t)}{\partial t^2} + c \frac{\partial \dot{u}(x, t)}{\partial t} + EI \frac{\partial^4 u(x, t)}{\partial x^4} - T \frac{\partial^2 u(x, t)}{\partial x^2} = \sum_{n=1}^{N} f_n + \sum_{n=1}^{N} I_n, \tag{9}$$

where m, c, EI, and T are the mass per unit length, viscous damping per unit length, elasticity, and tension distributions of the tape. $u(x, t)$ is the transverse displacement due to beam deformation. f_n and I_n are the frictional force between the tape and guide and tape–guide impact force at each constraint location, n, with N being the number of constraints in the system [13]. Using Eq. (8), Eq. (9) can be written as

$$m\ddot{u} + c\dot{u} + EIu'''' - Tu'' = \sum_{n=1}^{N} f_n + \sum_{n=1}^{N} I_n - m(\ddot{u}_g(x, t) + \ddot{u}_h(x, t)). \tag{10}$$

The nonlinear impact forces at the constraints are represented by

$$I_n = \begin{cases} -\lambda \delta(x - x_n)[\bar{u}(x_n, t) - s] & \text{if } \bar{u}(x_n, t) \geq s, \\ 0 & \text{if } s > \bar{u}(x_n, t) > -s, \\ -\lambda \delta(x - x_n)[\bar{u}(x_n, t) + s] & \text{if } \bar{u}(x_n, t) \leq -s, \end{cases} \tag{11}$$

where λ is the stiffness of the constraint. Typically this value is chosen to be approximately $100\times$ the stiffness of the system. In this study, that value was determined to be 1×10^6. Note that this value is dependent upon the solving method, in particular the time step used since changing the time step will

alter the magnitude of the mass and stiffness matrices. x_n is the x position of the constraint, n, and s is the clearance between the tape and guide. During solving, the overall displacement must be compared to the constraint clearance to determine whether tape–guide impacts will occur at each constraint.

To solve the nonlinear Eq. (10), mode superposition method is used. The tape displacement is expressed by

$$u(x, t) = \sum_{i=1}^{M} q_i(t)\phi_i(x), \tag{12}$$

where $q_i(t)$ is the modal amplitude of the ith mode and $\phi_i(x)$ represents the ith normalized mode. M is the number of modes used. Multiplying each side of Eq. (10) by $\phi_j(x)$, integrating over the length of the tape, and substituting Eqs. (6), (7), and (12), the following nonlinear differential equation governing the modal amplitudes is obtained:

$$\sum_{i=1}^{M}[m_{ij}\ddot{q}_i(t) + c_{ij}\dot{q}_i + (k_{ij} + t_{ij})q_i(t)] = \overline{f_{jn}} + \overline{I_{jn}} + \overline{A_{jg}} + \overline{A_{jh}}, \tag{13}$$

where $j = 1, 2 \ldots M$. The values of each element is given by Eqs. (14)–(22).

Modal mass, damping, stiffness, and tension elements are

$$m_{ij} = \int_0^L m\phi_i(x)\phi_j(x)\,\mathrm{d}x, \quad c_{ij} = \int_0^L c\phi_i(x)\phi_j(x)\,\mathrm{d}x, \tag{14,15}$$

$$k_{ij} = \int_0^L EI\phi_i''(x)\phi_j''(x)\,\mathrm{d}x, \quad t_{ij} = \int_0^L T\phi_i'(x)\phi_j'(x)\,\mathrm{d}x. \tag{16,17}$$

Frictional and impact forces between the tape and guide are

$$\overline{f}_{jn} = \sum_{n=1}^{N} f_n\phi_j(x_n), \quad \overline{I}_{jn} = \sum_{n=1}^{N} -\lambda\phi_j(x_n)\gamma(\bar{u}(x_n, t)), \tag{18,19}$$

where $\gamma(\bar{u}(x_n, t))$ is

$$\gamma(\bar{u}(x_n, t)) = \begin{cases} [\bar{u}(x_n, t) - s], & \text{if } \bar{u}(x_n, t) \geqslant s, \\ 0, & \text{if } s > \bar{u}(x_n, t) > -s, \\ [\bar{u}(x_n, t) + s], & \text{if } \bar{u}(x_n, t) \leqslant -s. \end{cases} \tag{20}$$

Reel forces due to moving boundaries are

$$\overline{A_{jg}} = \int_0^L \Omega_g^2 ma_g\left(\frac{x}{L}\right)\sin(\Omega_g t)\phi_j(x)\,\mathrm{d}x, \tag{21}$$

$$\overline{A_{jh}} = \int_0^L \Omega_h^2 ma_h\left(1 - \frac{x}{L}\right)sin(\Omega_h t)\phi_j(x)\,\mathrm{d}x. \tag{22}$$

The initial conditions of the system are given by

$$q_j(0) = \frac{\int_0^L u(x,0)\phi_j(x)\,\mathrm{d}x}{\int_0^L \phi_j^2(x)\,\mathrm{d}x}, \quad \dot{q}_j(0) = \frac{\int_0^L \frac{\partial u(x,0)}{\partial t}\phi_j(x)\,\mathrm{d}x}{\int_0^L \phi_j^2(x)\,\mathrm{d}x}. \tag{23,24}$$

Eq. (13) can be rewritten as

$$\mathbf{M\ddot{q} + C\dot{q} + (K + T)q = R}, \tag{25}$$

where $\mathbf{M, K, C}$, and $\mathbf{T}$ are the mass, stiffness, damping, and tension matrices, respectively. $\mathbf{R}$ is the right-hand side of Eq. (13).

3.3. Central difference method solution procedure

Eq. (25) can be solved using a variety of methods. The explicit central difference method is used in this study [15]. The step-by-step solution is as follows

(A) *Initial calculations*:
    (1) Form $\mathbf{M, K, C}$, and $\mathbf{T}$ from Eqs. (14)–(17) (note that in this study, damping effects of the tape and friction between the tape and guides were ignored).
    (2) Initialize modal displacement, velocity, and acceleration, $^0\mathbf{q}\,^0\dot{\mathbf{q}}\,^0\ddot{\mathbf{q}}$.
    (3) Select time step, $\Delta t, \Delta t \geqslant t_{\mathrm{cr}} \approx 2/\omega_n(\max)$ where $\omega_n(\max)$ is the maximum natural frequency of the system under free vibration. Calculate integration constants

$$a_0 = \frac{1}{\Delta t}, \quad a_1 = \frac{1}{2\Delta t}, \quad a_2 = 2a_0, \quad a3 = \frac{1}{a_2}.$$

    (4) Calculate $^{-\Delta t}\mathbf{q} = {}^0\mathbf{q} - \Delta t\,^0\dot{\mathbf{q}} + a_3^0\ddot{\mathbf{q}}$ for first time step iteration.
    (5) Form effective mass matrix, $\hat{\mathbf{M}} = a_0\mathbf{M}$.
(B) *Each time step*:
    (1) Calculate effective loads at time t,

$$^t\hat{\mathbf{R}} = {}^t\mathbf{R} - ((\mathbf{K + T}) - a_2\mathbf{M})^t\mathbf{q} - (a_0\mathbf{M})^{t-\Delta t}\mathbf{q}$$

$$^t\mathbf{R} = \overline{I_{jn}} + \overline{A_{jg}} + \overline{A_{jh}}.$$

    (2) Solve for displacements at time $t + \Delta t$, $\hat{\mathbf{M}}^{t+\Delta t}\mathbf{q} = {}^t\hat{\mathbf{R}}$.

Using this central difference method and applying the modal equations to the differential equation of motion, the vibration of the system can be calculated for any tape tension, thickness, speed, reel tilt amplitude, and constraint clearance.

4. Simulation

4.1. Modal analysis of magnetic tape

Free vibration of the system was investigated first. The tape was excited by an initial lateral velocity of 4 m/s at the guide. The effects of tape tension, thickness, and tape–guide clearance were studied. For all tests, Young's modulus of the tape was 7×10^9 GPa [16]. The tensions used were 0.5 N, 1 N, and 1.5 N. Currently, 1 N is the industry standard, thus, that was the nominal tension used in this study. The tape thickness was set at 9 μm for all tests in the effect of tension study. The values of β were solved for each mode and depended upon the tension and thickness for each test. The natural frequencies, ω, for each mode can be calculated from β using Eq. (4). Table 1 shows the test values used in the tension parametric study along with the first 10 calculated natural frequencies. For all tests, the first 10 modes were used for analysis, except in Section 4.3.2.1 when the effect of number of modes is studied for the case of two moving boundaries.

Table 2(a) shows the different values of I and m due to changing thickness of 6.5, 9, and 14.4 μm. These values correspond to industry tapes used in commercial drives. The current standard is 9 μm, thus it is the nominal tape thickness chosen for this study. The 6.5 μm thick tapes are smoother and will be used in future tape drives while 14.4 μm thick tape is outdated by several years, but is included for comparative analysis. For the effect of tape thickness the tape tension is 1 N. The values of β for each mode must again be recalculated and new values of natural frequency can be solved for. See Table 2(b) for the first 10 modal natural frequencies.

The second investigation involves moving the boundaries to simulate reel effects on the tape vibration according to Eqs. (6) and (7). a_h and a_g are the left and right reel tilt amplitudes, respectively. Ω_h and Ω_g are the left and right reel rotational frequencies based on the tape speed, V, and tape pack radius at each reel, R_{hg}:

$$\Omega_{hg} = \frac{V}{R_{hg}}. \tag{26}$$

Table 1
Calculated natural frequencies, in Hz, for effect of tension study. $E = 7 \times 10^9$ GPa, $I = 1.5178 \times 10^{12}$ m^4 (thickness = 9 μm), $m = 1.588$ kg/m

Mode	0.5 N	1 N	1.5 N
1	132.18	146.02	158.53
2	343.20	363.83	383.27
3	654.14	677.79	700.62
4	1066.68	1092.02	1116.78
5	1581.50	1607.90	1633.87
6	2198.83	2225.94	2252.73
7	2918.77	2946.40	2973.78
8	3741.40	3769.43	3797.23
9	4666.74	4695.07	4723.21
10	5694.82	5723.37	5751.79

Table 2

Properties	6.5 μm	9.0 μm	14.4 μm
(a) *Material properties used to calculate natural frequencies for effect of tape thickness study*[1]			
m	1.1469E-04	1.5881E-04	2.5409E-04
I	1.0962E-12	1.5179E-12	2.4286E-12

(b)*Calculated natural frequencies, (in Hz)*[1]			
Mode	6.5 μm	9 μm	14.4 μm
1	155.74	146.02	135.79
2	378.88	363.83	348.48
3	695.42	677.79	660.13
4	1111.12	1092.02	1073.08
5	1627.91	1607.90	1588.14
6	2246.58	2225.94	2205.64
7	2967.48	2946.40	2925.71
8	3790.83	3769.43	3748.43
9	4716.73	4695.07	4673.84
10	5745.25	5723.37	5701.98

[1]$E = 7 \times 10^9$ GPa, $T = 1$ N.

First the effect of only one reel will be studied by moving the left boundary and keeping the right one fixed. The effect of changing the linear tape speed, thereby changing the reel rotational speeds, will be studied with both boundaries in motion. Finally the effect of varying the reel-tilt amplitude will be studied. One test will also be performed that includes the effect of all 4 guides on the vibration of the system due to moving boundaries.

4.2. Transient analysis

To verify that the model can actually simulate vibro-impact, a simple test case was performed. The following values were used in this test: $E = 1 \times 10^{11}$ GPa, $I = 8.33 \times 10^{-6}$ m⁴, $T = 0$, and $L = 10$ m. One constraint is placed at $L = 5$ m and at a clearance of 500 μm. An initial velocity of 10 m/s was applied at $L = 5$ m to excite the beam. Fig. 5 shows the time history of the beam. Fig. 5(a) shows the vibration response with the constraint absent. As clearly shown, the beam easily vibrates past 500 μm. However, once the constraint is included in the system, Fig. 5(b), the vibration is effectively constrained at that point.

4.2.1. Free vibrations
4.2.1.1. Nominal conditions. The first test performed with actual tape values was the nominal condition of 1 N, 9 μm tape thickness, and clearance of 38 μm. According to a study by Goldade and Bhushan, tape width can average 12.649 mm for magnetic tapes typically used for experimental testing [9]. The guide clearance for a typical experimental tape drive is approximately 12.725 mm. Thus the average clearance would be at most, 38 μm, thus this is
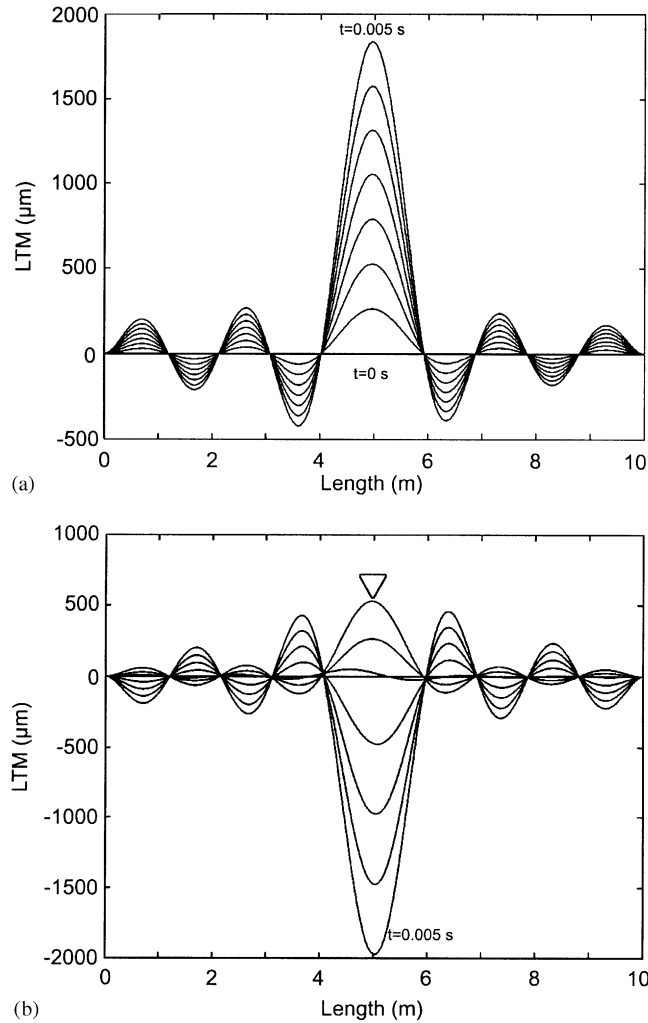
Fig. 5. Test case to verify effect of a constraint on LTM. $E = 1 \times 10^{11}$ GPa, $I = 8.33 \times 10^{-6}$ m^4, $T = 0$ N, $L = 10$ m. (a) Time history plot showing beam vibrations with no constraint. (b) Time history plot showing vibration due to rigid constraint of 500 μm, illustrating that the model is capable of simulating the effect of a rigid guide on lateral tape motion.

chosen as the nominal condition of tape–guide clearance throughout the study. Values for experimental tapes and drives are used because model results are compared to actual experimental data.

Fig. 6 shows the LTM and resulting frequency components of the tape under free vibration at nominal conditions. Note that the vibrations do not dissipate since the model neglects tape damping. As shown in Fig. 6(a), the constraints prevent any vibration past the clearance at the guides. At the head, Fig. 6(b), where there are no constraints, the LTM can vibrate at higher amplitude. The frequency plots are interesting to examine since the high-frequency peaks Figs. 6(c) and (d) correspond to the calculated values in Table 1, particularly for modes 5–10. The
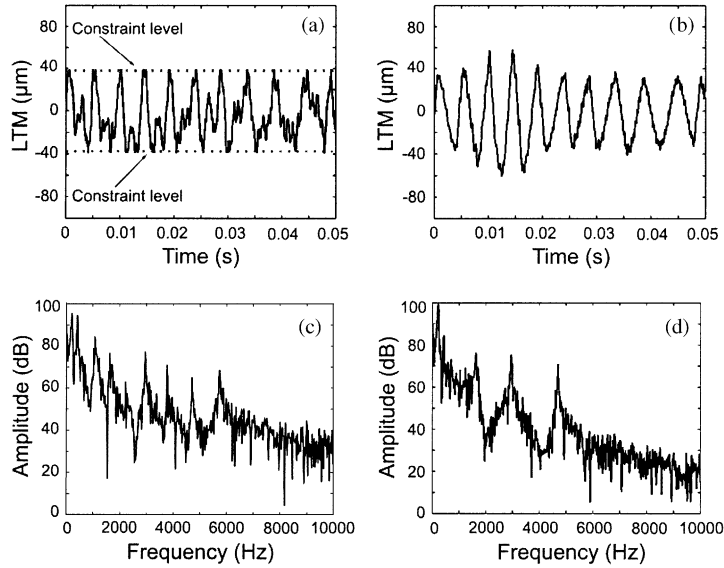
Fig. 6. LTM due to free vibration at nominal conditions. $T = 1\,\text{N}$, 9 μm thick tape, clearance = 38 μm, initial velocity, 4 m/s at the guide. (a) LTM at the guide is limited to the constrained clearance. (b) LTM at the head is unconstrained. (c) Frequency response of the LTM at the guide shows peaks above 1600 Hz correspond to calculated values (Table 1) while lower frequencies do not correspond as well due to the nonlinear nature of the vibratory system. (d) Frequency response of LTM at the head shows fewer vibratory modes.

lower modal frequencies, however, do not match the calculated values as closely. This is to be expected due to the nonlinearity of the system because the presence of a constraint is much more likely to interfere with the lower modal vibrations. Lower modes typically are associated with higher vibration amplitude, so if the amplitude is large enough, those modes will cause vibration sufficient to simulate guide impacts, thereby affecting the frequency of the signal. Future testing should include running the model for longer time steps to generate LTM plots of longer time length in order to more completely study the frequency effects since low-frequency data requires longer capture times.

4.2.1.2. Effect of tape tension.   Ideally, tape tension in a linear tape drive should be constant. In reality, however, tension transducers must constantly monitor tape tension and adjust the reel rotation speed accordingly in order to keep the tension as constant as possible. Thus, there will always be slight variations in actual tape tension. However, these variations can normally be ignored, leading to the assumption that tension is assumed to be constant and uniform in the tape. Fig. 7(a) shows the effect of tension on LTM at the head. According to Table 1, as tension increases, the natural frequency of the system should also increase. It is clear to see from the graph that at 1.5 N, the frequency is higher. The 1 and 0.5 N cases are both at lower frequencies, but it is not clear which is lower. Thus the trend predicted in Table 1 appears to hold in that as tension increases, frequency increases as well. Also, note that at time = 0.022 s, the 0.5 N tension LTM amplitude is approximately 30 μm higher than that of 1.5 N.
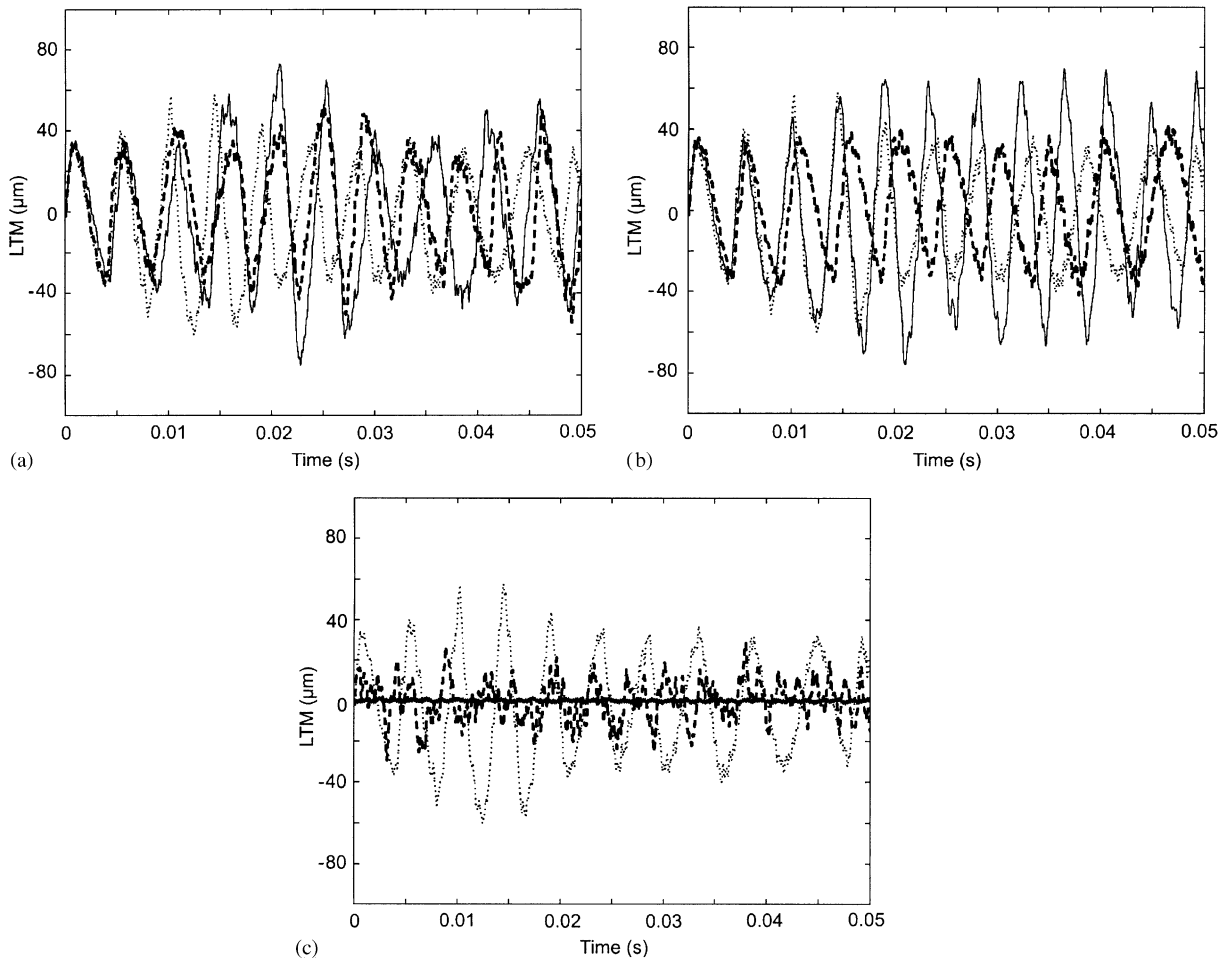
Fig. 7. Effect of tension, tape thickness, and tape–guide clearance on LTM. Measurement location: head, Initial velocity: 4 m/s at the guide. (a) Effect of tension: 1.5 N (---), 1 N (...), and 0.5 N (___), 9 μm thick tape, clearance = 38 μm. (b) Effect of tape thickness: 14.4 μm (---), 9 μm (...), and 6.5 μm (___), 1 N, clearance = 38 μm. (c) Effect of tape–guide clearance: 38 μm (---), 19 μm (...), and 3.8 μm (___) 1 N, 9 μm thick tape.

4.2.1.3. Effect of tape thickness. Fig. 7(b) shows the effect of tape thickness on LTM at the head. Table 2(b) shows that as thickness increases, the natural frequencies should decrease. It is obvious that at 14.4 μm, the frequency is lower than the other two cases. Also of interest to note is that the LTM amplitude is lower for the thicker thicknesses. Boyle and Bhushan [12] showed that thicker experimental tapes exhibited much higher LTM amplitude than the thinner tapes. This difference can be explained by realizing that tape–guide friction is neglected in this study and that newer tapes are smoother. Smoother tapes would have a higher real area of contact between the head and guides, increasing friction and possibly damping much of the LTM for thinner tapes. Thicker and older tapes would be rougher, causing less friction between the tape and guides, allowing much higher tape LTM. These effects, however, could not be studied in the absence of tape–guide friction. Also, tape edge quality has been shown to have significant impact on LTM [9,10,12].

Thus the experimental tapes used in experimental studies may have tape edge characteristics that can increase or decrease LTM. The thicker tapes would typically be found to have rougher edges which could lead to high lateral motion.

4.2.1.4. Effect of tape–guide clearance. Fig. 7(c) shows the effect of changing the tape–guide clearance on LTM at the head. As previously discussed, the nominal clearance is 38 μm. The other values used were 19 and 3.8 μm corresponding with one-half and one-tenth of the nominal clearance. Tape–guide impacts would be similar to applying periodic impulse loads to the tape edge. These impulse loads would be expected to cause higher-frequency behavior in the tape. At 19 μm, the signal amplitude is lower, but it is clear that the signal becomes more unstable as more impact events occur between the tape and guide. With repeated impacts, tape edge damage can occur, further degrading the tape edge, possibly leading to more severe LTM. Modern tape drives utilize head tracking servos to compensate for low-frequency LTM. By constraining the guides more, lower LTM can be achieved, but at the cost of introducing higher-frequency components into the system and damaging the tape edge. Thus a balance must be found that minimizes LTM amplitude yet allows adequate head tracking compensation and tape edge quality.

4.3. Forced vibrations (moving boundaries)

4.3.1. Effect of one moving boundary
Fig. 8(a) shows the LTM at the guide for the case of a moving boundary condition at the left boundary (see Fig. 4). Two simulations were run at different reel tilt amplitudes of 75 and 150 μm. Nominal conditions for tape tension, thickness, and tape–guide clearance was used. Since 75 μm is less than the clearance of the guides (76 μm = 2 s), it is expected that no tape–guide impacts occur. The beam is simply forced into harmonic motion at a frequency of Ω_h, the reel rotational frequency which is equal to 48 Hz for a tape speed of 6 m/s and tape pack radius of 0.02 m. At a reel tilt amplitude of 150 μm, however, the tape contacts the guide many times as the boundary moves. Since there is no damping in the system, the effects of each subsequent tape–guide impact progressively makes the LTM more severe as time progresses.

Fig. 8(b) shows the LTM at the head for the same test conditions as the previous figure. Interesting to note is that in previous simulations (see Figs. 6 and 7), at a position further from the moving boundary, the LTM is lower. In Fig. 8(b) however, the LTM amplitude is actually smaller at the head compared to the guides. So while the tape was forced into LTM of greater than 38 μm at the guide, by the time the effect of the guide reached the head, the magnitude was lessened. These effects would be further exaggerated with the presence of damping and tape–guide frictional forces.

Two time history plots are presented in Figs. 8(c) and (d). The constraint is also superimposed on the graph for further clarification. The top plot shows that while at the reel, the displacement is very near 38 μm, at the guide, the displacement is much lower. Thus no impacts occur. In Fig. 8(d), it is clear to see that with reel tilt amplitude increased, vibration at the guide is constrained.

4.3.2. Effect of two moving boundaries
4.3.2.1. Nominal conditions. Once it was established that the model could predict vibration response due to one moving boundary, tests involving both boundaries moving were performed
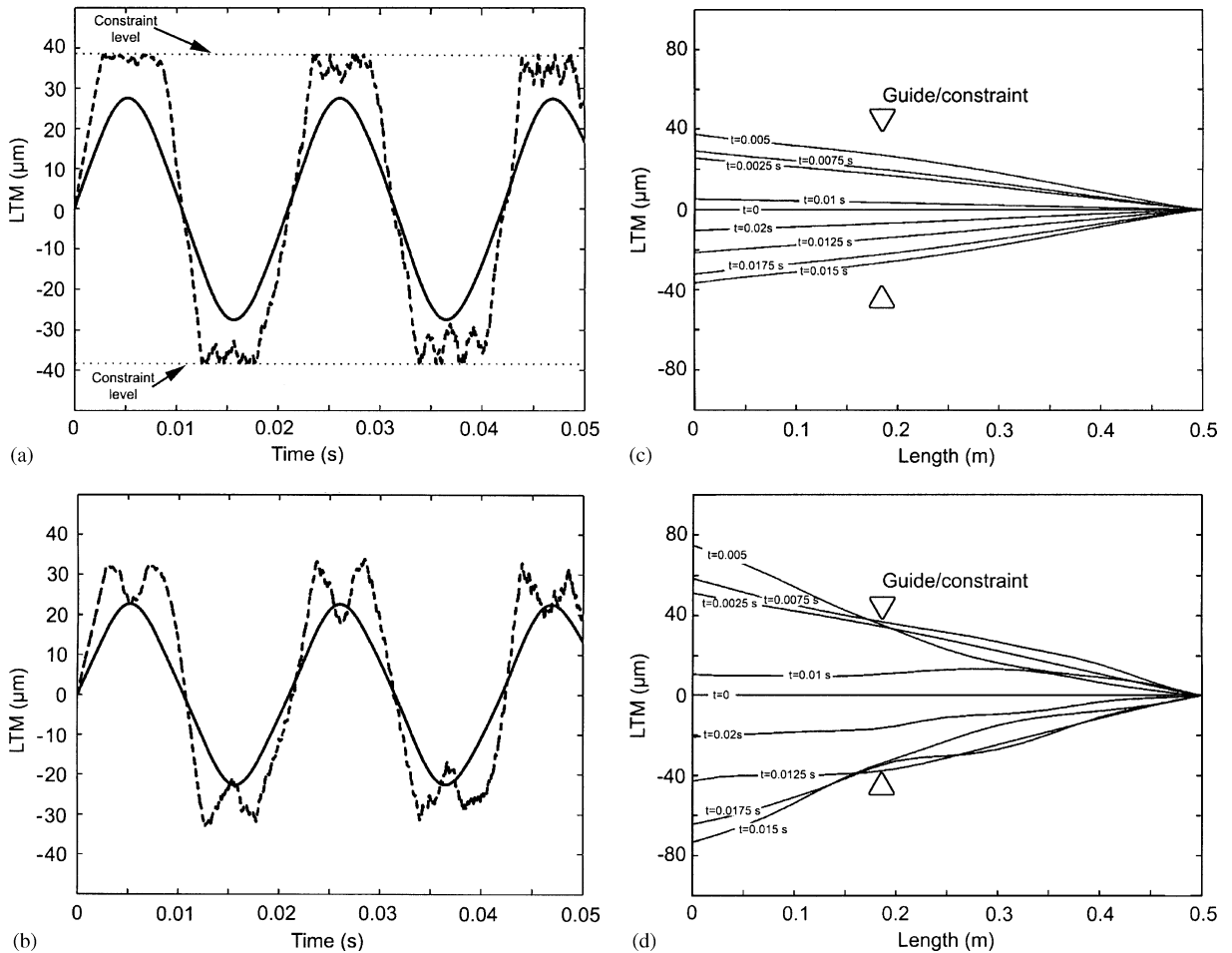
Fig. 8. Effect of reel tilt with one moving boundary. $T = 1$ N, 9 μm thick tape, clearance $= 38$ μm. (a) Measurement location: guide. Left reel tilt amplitudes of 150 μm (- - -) and 75 μm (___). Note that at higher reel tilt amplitude, the tape is effectively constrained by the guide. (b) Measurement location: head. Left reel tilt amplitudes of 150 μm (- - -) and 75 μm (___). (c) Time history plot showing tape vibration along the tape length at 0.0025 s time intervals, left reel tilt = 75 μm. (d) Time history plot showing tape vibration along the tape length at 0.0025 s time intervals, left reel tilt = 150 μm.

(simulating the effect of both reels under different degrees of reel tilt amplitudes). Nominal conditions for reel tilt amplitude for each reel is 75 μm, but the rotational reel frequencies for each reel, Ω_h and Ω_g equal 48 and 64 Hz, respectively. At these conditions, a study was made on the effect of the number of modes used by the model. Fig. 9(a) shows the effect of number of modes on LTM at the guide at nominal conditions. Actual LTM contains both low and high-frequency components. The number of modes used in the model determines the frequency range of the simulated LTM. Thus enough modes should be used in the simulation to generate signals that will more accurately resemble experimental data. It is clear that as the number of modes increases, the simulated LTM signal is improved. That is, by using fewer modes, the signal is very smooth,
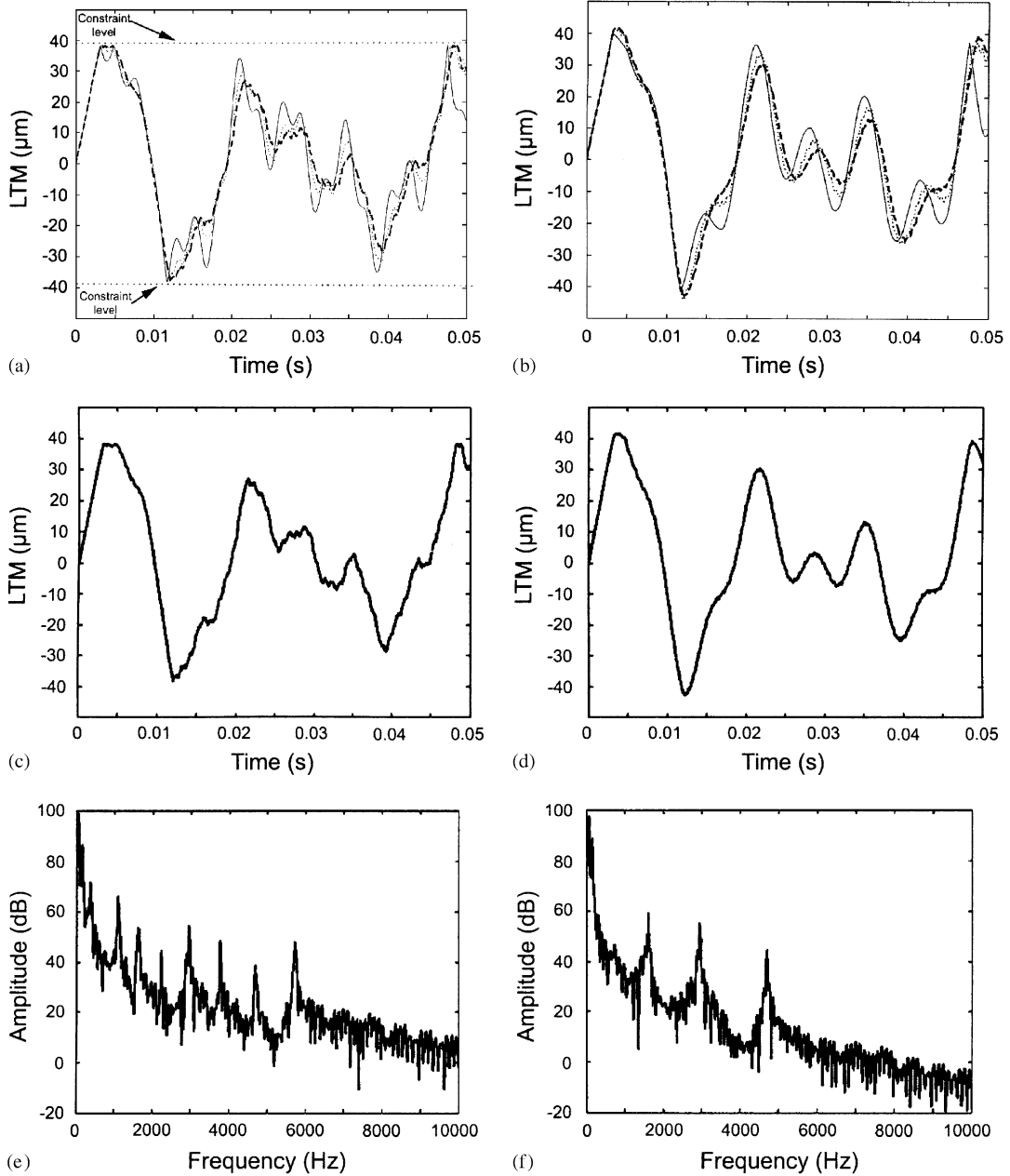
Fig. 9. LTM at nominal conditions with two moving boundaries; $T = 1$ N, 9 μm thick tape, clearance $= 38$ μm, left/right reel tilt amplitude $= 75$ μm. (a) Effect of number of modes: 10 modes (- - -), 5 modes (. . .), and 3 modes (___), measurement location: $=$ guide. (b) Effect of number of modes: 10 modes (- - -), 5 modes (. . .), and 3 modes (___), measurement location: head. (c) LTM (10 modes) at guide. (d) LTM (10 modes) at head. (e) Frequency response (10 modes) at guide. (f) Frequency response (10 modes) at head. Frequency peaks correspond to calculated values in Table 1.

showing mostly low-frequency content. As more modes are used in the simulation, the higher-frequency data (caused by vibro-impacts with the constraint), indicated by the smaller and more frequent spikes in the signal, can be observed. It is debatable whether 5 modes are enough, but it is clear that at 3 modes or less, the signal is too smooth to yield sufficient high-frequency simulation data that corresponds well enough with measured LTM. Fig. 9(b) shows a corresponding plot of LTM at the head. The LTM signal is much simpler at the head, so the number of modes might not be so critical at this measurement position, though 3 modes still looks insufficient. Figs. 9(c–f) show the nominal condition LTM at both the head and guide for 10 modes. As was the case in Figs. 6(c) and (d), the frequency peaks match those calculated in Table 1 for nominal conditions. At the head, the natural frequencies associated with the lower modes are not clearly visible due, likely, to the nonlinearity of the system (due to the presence of the rigid constraints). Future testing should include running the model for longer time steps to generate LTM plots of longer time length in order to more completely study the frequency effects since low-frequency data requires longer capture times.

4.3.2.2. Effect of speed. The next test involved varying the linear tape speed. This has the effect of changing the reel rotational frequencies, and thus altering the moving boundaries. In actual tape drive operation, the tape pack radius continually changes as the tape winds and unwinds. Thus the reel rotational frequencies change continuously as well. In this study, the model time durations used were too small for noticeable changes in tape pack radius, thus the tape pack radii were constant for each test. Fig. 10(a) shows that as tape speed increases, the frequency of the system also increases. It is unclear from this scale whether tape speed actually affects LTM amplitude or not.

4.3.2.3. Effect of reel tilt amplitude. To investigate how reel tile amplitude affects LTM, the right reel tilt amplitude was kept at 75 μm while the left reel tilt amplitude was set to 10, 75 and 150 μm. The results are shown in Fig. 10(b). It is clear that at 10 μm, there is not enough reel-induced displacement to cause significant tape–guide impact. Displacement (150 μm), compared to 75 μm displacement, shows much more erratic LTM behavior, though the amplitude is very similar. The effect of damping and tape–guide frictional forces would likely affect these results quite a lot since the effects of the reels would be further diminished down the length of the tape.

4.4. Simulation of 4 constraints

The final test case involved studying the effect of having all 4 guides accounted for in the model, subjected to moving boundaries. The same reel rotational frequencies were used as above, but the left reel tilt amplitude was set to 75 μm and the right reel tilt amplitude was set to 1 μm to investigate the simpler case of only one moving boundary having high reel tilt amplitude. Nominal conditions were used at all other values. Fig. 11(a) shows that guide 1 (see Figs. 3 or 11(c)) is forced against the constraint almost all the time. This makes sense considering that guide is very near the left reel and subjected to very high displacement. Guide 2 experiences some tape–guide impact, but not as much as the first guide since the LTM is much more reduced by this point. Further down the tape path, guides 3 and 4 experience no tape–guide impacts at all. If the right reel tilt amplitude was higher, higher amplitude would be expected. It is clear though, that the
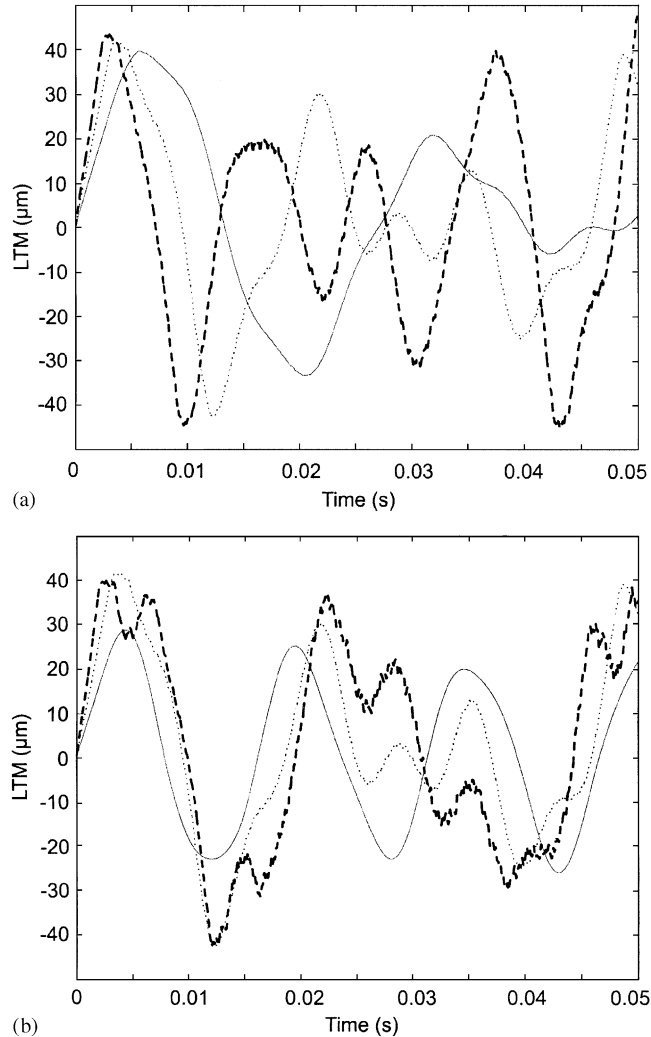
Fig. 10. (a) Effect of speed on LTM with two moving boundaries: 8 m/s (- - -), 6 m/s (. . .), and 4 m/s (___), 1 N, 9 μm thick tape, clearance = 38 μm, left reel tilt = right reel tilt = 75 μm, measurement location: head. (b) Effect of reel tilt on LTM with two moving boundaries: 150 μm (- - -), 75 μm (. . .), and 10 μm (___), 1 N, 9 μm thick tape, clearance = 38 μm, velocity = 6 m/s, right reel tilt amplitude = 75 μm, measurement location: head.

more critical guides to suppress LTM are the ones nearest the reels. Fig. 11(b) examines the LTM at the head location for 4 guides and compares that to the LTM at the head for the nominal case and only 1 guide. It is clear to see that with 4 guides the motion is much more complex, yet the amplitude is very similar. What is very interesting to note is that in the single constraint case, the right reel tilt amplitude was 75 μm, while in the case of multiple constraints, the right reel tilt amplitude was only 1 μm. Thus, even though the moving boundary is lower in the 4 guide case, the amplitude is nearly the same. Fig. 11(c) shows a time history plot with all 4 guides superimposed for clarity. It is very easy to see that at guide 1, the LTM is very constrained, yet at the other
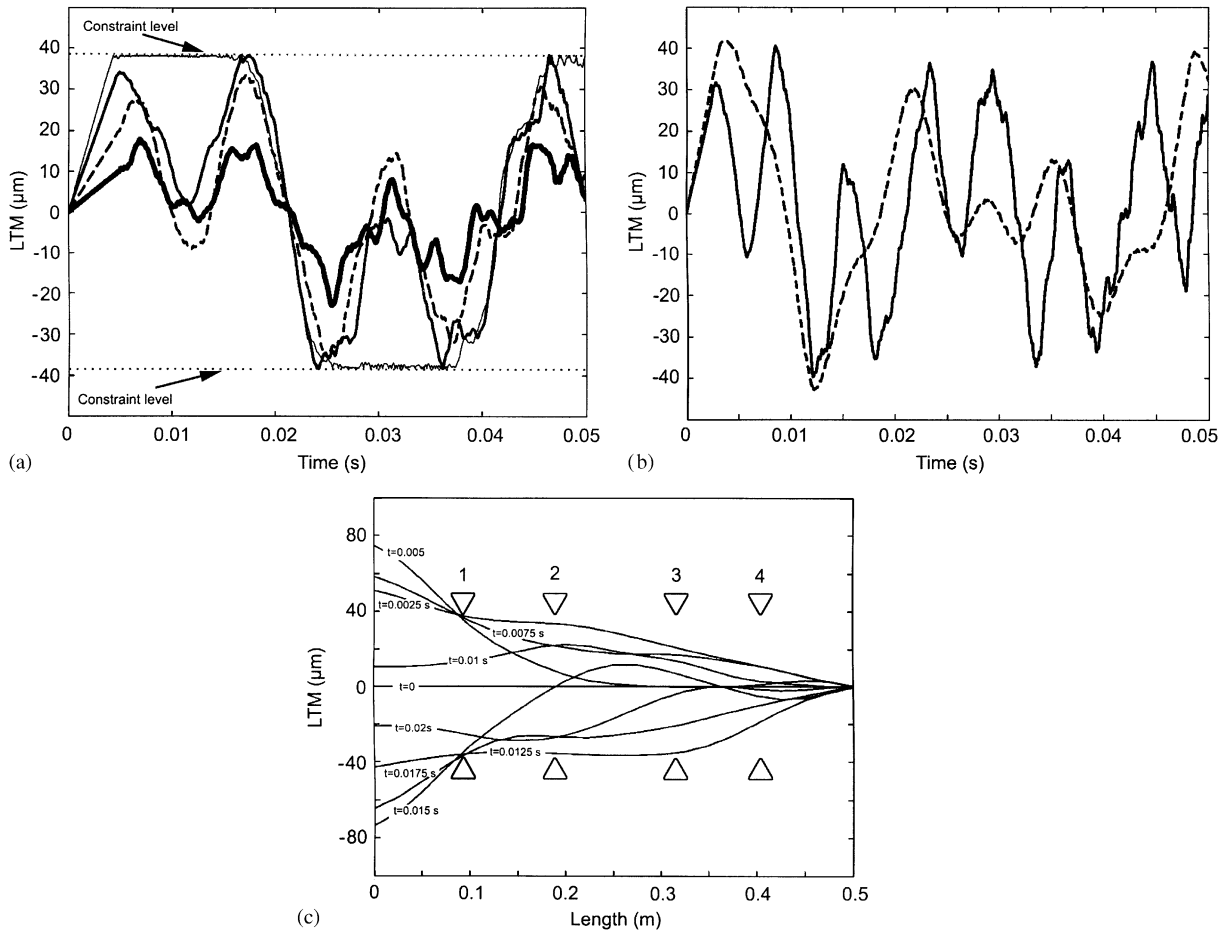
Fig. 11. Simulation of vibrating tape with two moving boundaries (right/left reel tilt = 75 μm/1 μm), 1 N, 9 μm thick tape, clearance = 38 μm. (a) LTM at each guide: guide 4 (▬▬▬), guide 3 (---), guide 2 (———), and guide 1 (___). (b) LTM comparison at the head for 1 guide/constraint (---) vs. 4 guides/constraints (___). (c) Time history plot showing tape vibration along the tape length at 6 m/s. Constraints also shown for further illustration.

guides, there is hardly any impact at all. It is easy to envision a case with higher right reel tilt amplitude having much more tape–guide interaction.

Further simulations should be run at more realistic conditions including tape damping, tape–guide friction, and with the presence of staggered wraps, but it can be inferred that minimizing reel tilt amplitude and optimizing the guide clearance is very critical to tape vibration. Tight clearances will minimize LTM, especially at the guides nearest the reels, but this will result in possible tape edge damage and higher-frequency LTM that cannot be adequately compensated by the head tracking servos. Higher clearances will minimize tape edge damage but higher LTM amplitude will result, which could be difficult to compensate for. It is possible that adjusting the clearance for each guide along the tape path could provide an optimum guiding system to minimize LTM most effectively, but further simulation will be required.

4.5. Comparison with experimental data

Fig. 12 shows actual experiment LTM data taken in a previous study [12]. Note that in the study of tape speed, no noticeable trends were visible, but in Fig. 12(a), it appears that at higher speeds there is higher LTM amplitude. This can be due to several reasons. At higher speeds, the frictional force between the tape and guide could be lessened, allowing more motion to occur than at lower speeds when the frictional force might be higher. Also, the effect of speed could also be dependant upon the reel operation. At higher speeds, the reels undergo higher-frequency rotational behavior than at lower speeds, possibly causing a higher LTM signal.

Fig. 12(b) shows the effect of tape tension. It is very difficult to see any trends when tension is changed, but according to the calculations, the frequency should increase slightly with tension. Fig. 7(a) shows that at the highest tension tested, frequency does indeed slightly increase, but it is difficult to compare the experimental data to the model due to the lack of damping and frictional forces. Future work would include more detailed frequency analysis than was performed in this study.
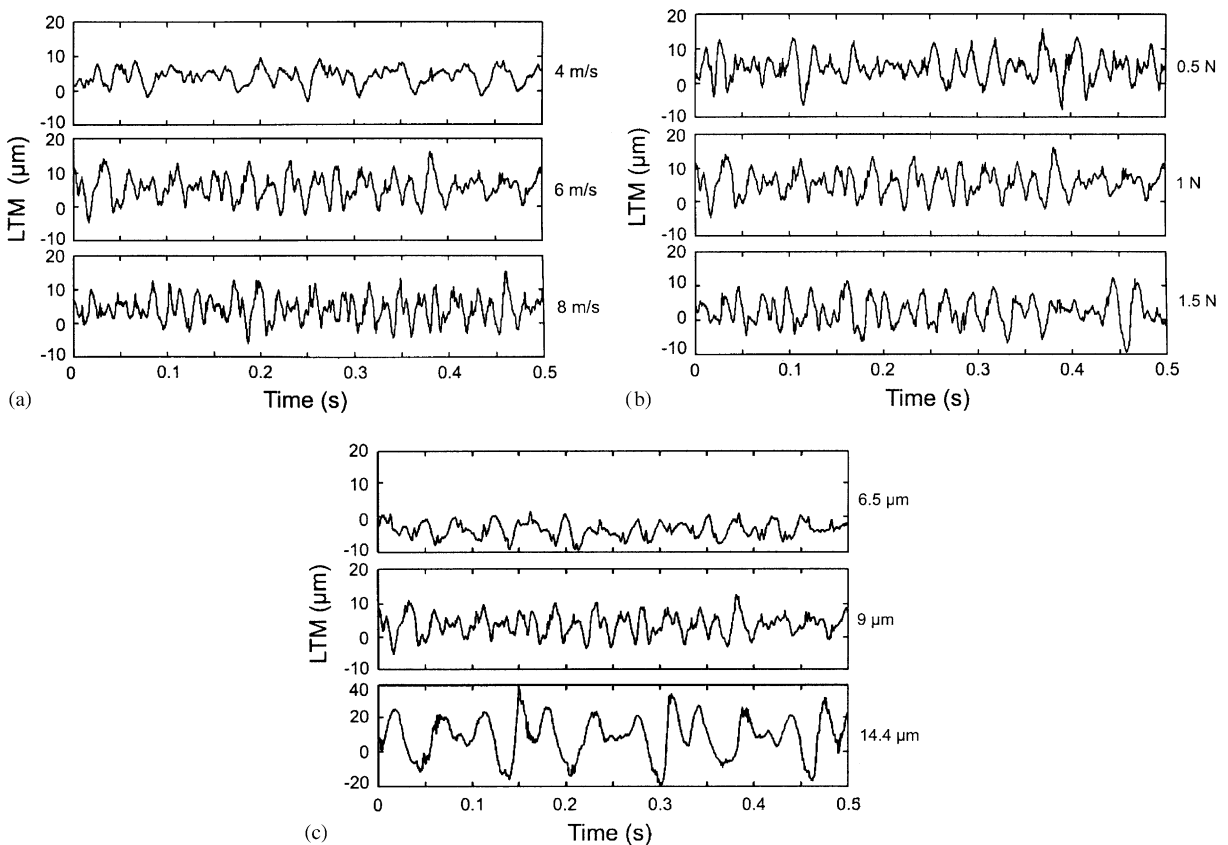

Fig. 12. Actual experimentally measured LTM near the head. (a) Effect of tape speed (1 N, 9 μm). (b) Effect of tension (6 m/s, 9 μm). (c) Effect of tape thickness (6 m/s, 1 N) [12].

[Fig. 12](c) shows the effect of tape thickness. As in the model, the thicker tape has a lower frequency. However, contrary to the model, the 14.4 μm tape has much higher LTM amplitude. This can be due to several reasons. The 6.5 μm tape is relatively new and of much higher quality and smoothness. The 14.4 μm is several years old and was only used to provide a comparison with the other thicknesses. Also, tape edge quality was ignored in the model but could significantly affect LTM. The experimental data clearly shows that 14.4 μm exhibits the highest LTM. This can be explained if the roughness of the tape is high enough that the friction between the tape and guide is lessened, allowing much more LTM than the smoother thinner tapes. It could also be explained if the thicker tape has an unfavorable tape edge that resulted in increased LTM. What is very interesting to note, however, is that the maximum LTM values of the experimental data are near 38 μm. This corresponds very well to the expected clearance in the tape drive used to take the data.

5. Conclusions

5.1. Free vibration conclusions

(1) The model calculates relatively accurate results since the calculated natural frequencies match up well with the frequency peaks observed in testing.
(2) As tape thickness increases, the natural frequency decreases a bit, just as predicted. This is the same trend observed in experimental testing. The LTM amplitude trends are different. For thicker tape, the model showed lower LTM amplitude, while the experimental results show that the thicker tape has much higher LTM. This can be due to poor tape edge quality in the older thicker tapes.
(3) As tape clearance is lowered, lateral tape motion, LTM, amplitude also lowers since it is more constrained, but the effect of so many simulated vibro-impacts yields a signal with much higher-frequency content. Lowering clearance might decrease the LTM amplitude, but it could pose a problem if head tracking servos are not able to compensate for the resulting higher-frequency motion.

5.2. Forced vibration conclusions

(1) The effect of one moving boundary shows that reel effects can be modeled in the system. Future work would include adding an expression for staggered wraps and would be superpositioned with the reel tilt amplitude.
(2) Reel tilt amplitude has a large effect on tape guiding. Future work would include expanding the equation describing the reel motion by adding expressions for reel runout, reel imperfections, and change in tape pack radius.
(3) When all 4 constraints were modeled, it was shown that even though the left/right reel tilt amplitudes were 75 μm/1 μm, respectively, the resulting LTM amplitude at the head was nearly the same as for the nominal case with only 1 guide with left/right reel tilt amplitudes of 75 μm/75 μm. It is clear to see that the actual case of 4 guides is a much more complicated system that could be studied in depth.

(4) For simplicity, this model did not simulate motion in the x direction (that is, simulate the tape moving from reel to reel), but in reality, there would be motion in that direction, likely causing even more impacts at the guides. Simulating this realistic tape motion is a more difficult problem theoretically, but would result in a more accurate model.
(5) As mentioned several times throughout this study, the effects of tape damping would be a good way to further add to the accuracy of the model, along with the friction force between the tape and guide (and head), and the effect of tape buckling.
(6) In this study, the tension was assumed to be constant. This is not the case in a real drive. As the tape vibrates, the tension would change, altering the vibration modes of the system. Future work could include taking into consideration the effects of varying tension during simulation.

Acknowledgements

References

[1] B. Bhushan, *Tribology and Mechanics of Magnetic Storage Devices*, second ed., Springer, New York, 1996.
[2] B. Bhushan, *Mechanics and Reliability of Flexible Magnetic Media*, second ed., Springer, New York, 2000.
[3] C.D. Mee, E.D. Daniel, Magnetic Recording Technology, *second ed.*, McGraw-Hill, New York, 1996.
[4] D.B. Richards, M.P. Sharrock, Key issues in the design of magnetic tapes for linear systems of high track density, *IEEE Transactions on Magnetics* 34 (1998) 1878–1882.
[5] R. Jewett, 1 kHz servo actuator threshold discussion, conversation, 2003.
[6] J.J. Topoleski, B. Bhushan, Qualitative and quantitative evaluation of the quality of factory-slit magnetic tape edges, *Journal of Information and Storage Processing Systems* 2 (2000) 109–116.
[7] B. Bhushan, P.S. Mokashi, Effects of cycling on debris propensity in a linear tape transport, *Journal of Information and Storage Processing Systems* 3 (2001) 267–275.
[8] S.J. Hunter, B. Bhushan, Debris propensity of magnetic metal particle tapes, *Journal of Information and Storage Processing Systems* 3 (2001) 143–159.
[9] A. Goldade, B. Bhushan, Measurement and origin of tape edge damage in a linear tape drive, *Tribology Letters* 14 (2003) 167–180.
[10] A. Goldade, B. Bhushan, Tape edge study in a linear tape drive with single-flanged guides, *Journal of Magnetism and Magnetic Materials* 271 (2004) 409–430.

[11] R. Taylor, P. Strahle, J. Stahl, M. Dugas, F. Talke, Measurement of cross-talk motion of magnetic tapes, *Journal of Information and Storage Processing Systems* 2 (2000) 255–262.

[12] J.M. Boyle Jr., B. Bhushan, Vibration response due to lateral tape motion and impulse force in a linear tape drive, *Microsystem Technologies* 11 (2005) 48–73.

[13] E. Emaci, T.A. Nayfeh, A.F. Valakis, Numerical and experimental study of nonlinear localization in a flexible structure with vibro-impacts, *Zeitschrift für Angewandte Mathematik und Mechanik* 77 (1997) 527–541.

[14] D.J. Gorman, *Free Vibration Analysis of Beams and Shafts*, Wiley, New York, 1975.

[15] K.J. Bathe, *Finite Element Procedures in Engineering Analysis*, Prentice-Hall, Englewood Cliffs, NJ, 1982.

[16] B. Bhushan, T. Ma, T. Higashioji, Tensile and dynamic mechanical properties of improved ultrathin polymeric films, *Journal of Applied Polymer Science* 83 (2001) 2225–2244.